Optimal Unmanned Aerial Vehicle Allocation for Border Surveillance

Volkan Sözen

Turkish Army
vsozen@kkk.tsk.tr

E. M. Craparo

Naval Postgraduate School
emcrapar@nps.edu

ABSTRACT

Border surveillance is an important concern for nations wishing to detect and intercept intruders. Unmanned aerial vehicles (UAVs) allow for modernization of border surveillance efforts, improving performance while reducing cost. While UAVs carry a number of advantages over traditional means of border surveillance, they also present new operational challenges. This paper formulates mathematical models designed to find the best way to utilize a given fleet of UAVs by deciding their routes, altitudes, and speeds in order to maximize the probability of detecting intruders. These models can aid a decision maker in effectively acquiring and employing a UAV fleet for border surveillance.

INTRODUCTION

The problem of defending a territory against intruders has existed for millennia, and modern nations face no shortage of potential intruders. These intruders can include terrorists, drug traffickers, smugglers, illegal immigrants, and others who represent a threat to national interests. A first step toward preventing intrusion is detecting potential intruders. While the problem of detecting intruders is not new, the ecosystem of threats and countermeasures continues to expand and evolve. Unmanned aerial vehicles (UAVs) represent one emerging tool in this domain. A variety of advantages motivate the use of UAVs for border surveillance: many UAVs can be controlled by a single operator, reducing personnel costs; they are very fast and can patrol large regions; and they have wider regions of view than conventional surveillance methods, thus potentially increasing the probability of detecting intruders. UAVs' mobile nature means that they can be deployed more flexibly and reconfigured more easily that many other forms of border surveillance, and it can also give them a stealth advantage. These advantages and others have made UAVs an important complement to human expertise in the border control domain (Preston, 2014). As noted by Haddah and Gertler (2010), there are two types of UAVs: autonomous drones and remotely piloted vehicles (RPVs). Both types are unmanned, but drones are preprogrammed for their flight and mission, whereas RPVs are actively controlled by an operator at the ground station. Both are good candidates for border surveillance, but both need good planning in order to realize their full potential.

This paper gives guidance to UAV operators and mission planners on how to optimally employ their UAVs while conducting surveillance on a border in order to maximize the probability of detecting intruders. Throughout the paper, we refer to UAVs as searchers and intruders as targets.

This paper is organized as follows. We first review a selection of the small but growing literature on the use of UAVs for border surveillance. We then consider a fundamental border patrol problem referred to as the "barrier patrol problem" by Wagner et al. (1999) and "patrolling a channel" by Washburn (2002). We derive a more accurate detection probability formula than currently exists in the literature and validate our formula using Monte Carlo simulation. Building upon this result, we expand our analysis to include multiple searchers. We determine the best way to allocate a border among multiple heterogeneous searchers, and we study the change in optimal allocation depending on the differences in the searchers' characteristics. Finally, we demonstrate a methodology for determining the optimal way to operate multiple searchers when the performance of the searchers' sensors degrades with increasing searcher speed. This methodology calculates both the allocation and speeds required to achieve the maximum detection probability.

BRIEF LITERATURE REVIEW

Although UAVs are relative newcomers to the border surveillance domain, efforts to analyze and optimize their operations predate their actual deployment. For example, Girard et al. (2004) propose a hierarchical control architecture for UAV teams, while Matveev et al. (2011) develop a guidance-control law to allow UAV with a fixed camera to follow and monitor a border in the presence of obstacles. Szechtman et al. (2007) compare the performance of a UAV to a stationary sweeping camera against intruders who appear according to a Poisson process in locations determined by a specified distribution. Ozcan (2013) takes a simulation-based approach to examine the effectiveness of

APPLICATION AREAS:
Unmanned systems, Homeland defense and civil support
OR METHODOLOGIES:
Optimization, Simulation

UAVs in a particular scenario. After performing a sensitivity analysis on various parameters, she concludes that the UAV's detection and classification performance as well as the target's counter-detection capabilities are the most important factors impacting detection probability.

A body of work also examines various sensor models, which are not the focus of this paper but are an important component of the search and detection problem. For example, Soza & Company (1996), Wagner et al. (1999), Washburn (2002), Sözen (2014), and Haddah and Gertler (2010) study lateral range curves and possible approximations of them. Additionally, Wagner et al. (1999) explains how lateral range curves are determined for a particular sensor. They perform preliminary analyses on the approximations, mentioning the differences between the actual sensor model and its approximations.

THE BORDER PATROL PROBLEM

We consider the basic problem of monitoring a straight-line border over flat terrain without any line-of-sight issues. Our hypothetical border is bounded by two barriers that are perpendicular to the border. These barriers may represent actual (physical) barriers or imaginary barriers denoting a region of interest. We have one or more searchers available and would like to employ them in such a way as to maximize our likelihood of detecting an entity attempting to cross the border; this entity is henceforth referred to as "the target." We assume that the target moves with constant speed perpendicular to and toward the border, while the searchers patrol the border by moving back and forth at constant speed, reversing direction instantaneously at the endpoints of their patrol regions. For simplicity, we assume that the target cannot see the searchers and takes no action to evade them. Future work may consider an intelligent target that can detect and evade the searchers.

Border Patrol with a Single Searcher

As a first step toward optimally deploying one or more searchers, we first determine the probability of detecting the target with a single deployed searcher. We assume that the searcher is equipped with a sensor capable of detecting the target within a finite radius. For simplicity, we consider a definite range or "cookie-cutter" sensor, meaning that if the distance between the target and the searcher is less than the detection radius, detection occurs with probability 1; otherwise, detection does not occur. Such a sensor represents an approximation of, for instance, a vision-based sensor operating in the absence of obstacles. Other sensor models are possible, and a similar analysis could be performed for sensors that are not oriented in a downward-facing posture, or sensors for which a definite range approximation is not appropriate.

Figure 1 illustrates our problem setup. The length of the border is L units, and the searcher moves back and forth along the border with constant speed v. The searcher's detection radius is R, and we assume that this radius dictates the searcher's trajectory along the border: when the searcher is at a distance of R units away from either edge of the border, it turns and moves in the opposite direction. A target attempts to pass through the border at constant speed u, and if the target's position is within distance R of the searcher's position at any point in time, the target is detected. Otherwise, it is not detected.

Analytical Model

In order to calculate the probability that the searcher will detect the target, we utilize *target-stationary geometry*. Target stationary geometry

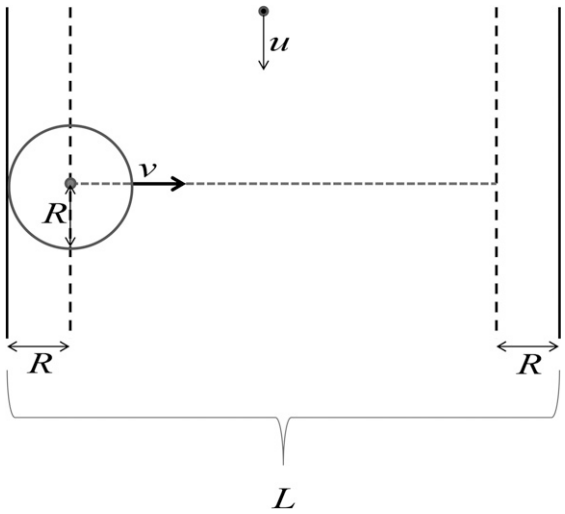

Figure 1. Simple border patrol problem setup.

uses a coordinate system that moves with the target rather than a stationary coordinate system (Eagle, 2013). To use target-stationary geometry, we simply add a vector $-u$ to every speed vector in our problem. That is, we add a vector with the same magnitude as the target's speed vector, but in the opposite direction. After performing the reference geometry transformation, the transformed speed of the target ($\tilde{u}$) is 0, and the transformed speed of the searcher ($\tilde{v}$) changes depending on the direction of the searcher's movement. In terms of our problem setup shown in Figure 1, if the searcher is moving to the right, its corresponding speed vector will be the vector shown in Figure 2(a). Likewise, if the searcher is moving to the left, its speed vector will change as shown in Figure 2(b).

Following this coordinate transformation, the border patrol problem shown in Figure 1 can be visualized as shown in Figure 3(a). In this figure, the searcher follows the dashed-dotted lines according to the speed vectors shown in Figure 2, and its detection radius is indicated by solid lines. Two targets, depicted as solid dots, are stationary. The searcher moves in the infinitely long region bounded by the two barriers. Thus, when using target-stationary geometry, the border patrol problem is transformed into a channel search problem in which the searcher looks for stationary targets in the infinitely long channel bounded by the barriers.

Figure 3(b) shows the detection region in the target-stationary case. If a target is in the shaded region, it is detected. Likewise, if it is not in the shaded region, it is not detected. In this example, target 2 from Figure 3(a) is detected, and target 1 is not.

Assuming a uniform target density, the probability of detection can be calculated as

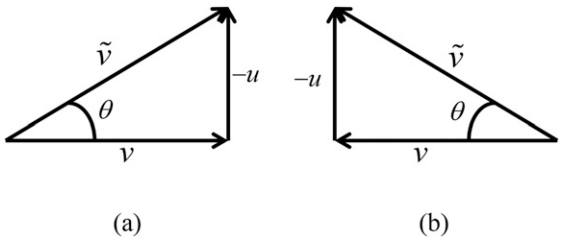

Figure 2. Transformed speed of the searcher in target-stationary geometry.

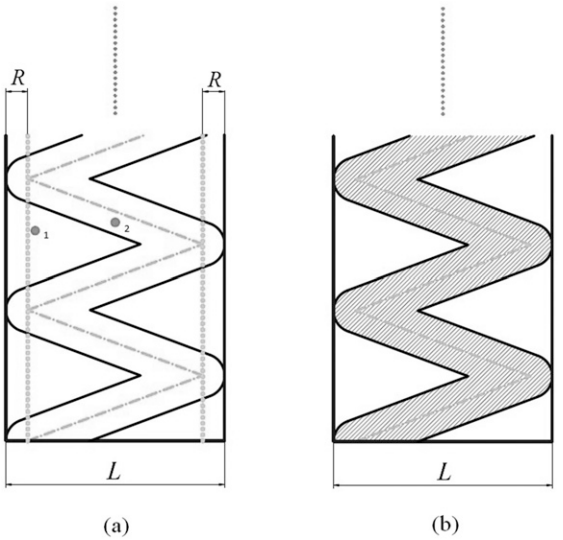

Figure 3. The border patrol problem in target-stationary geometry.

the ratio of the shaded area in the infinitely long channel to the area of the channel itself. As Figure 3(b) indicates, the shaded area follows a consistent pattern. In particular, between each of the searcher's turning points, the areas of the shaded regions are equal to each other. Moreover, the vertical distance between any two consecutive turning points is the same. Thus, we can calculate the detection probability by considering a region like that shown in Figure 4 (a), which is simply the region between two consecutive turning points. We can find the probability of detection by computing the ratio of the shaded area to the area of the outlined rectangle in Figure 4(a).

We calculate the area of the shaded region in Figure 4(a) by dividing it into separate regions as shown in Figure 4(b). The area of the shaded region inside the rectangle in Figure 4(b) can be found by calculating the areas of the two wedge-shaped regions on the ends of the region and the inner rectangle (shaded areas). By adding these two areas and

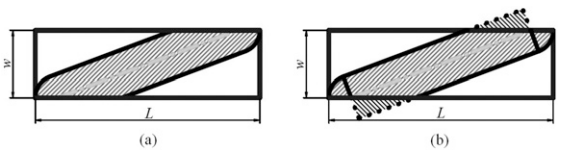

Figure 4. Area of coverage between two searcher turning points in target-stationary geometry.

subtracting the shaded regions outside of the rectangle, we obtain the area of the original shaded region.

Washburn (2002) determined an upper bound on this area by calculating the area shown in Figure 5(a). Wagner et al. (1999) arrived at a different approximation of this area by removing the regions lying outside the rectangle, as shown in Figure 5(b).

Using his approximation, Washburn (2002) obtains the following upper bound on the detection probability P_d:

$$P_d \leq \min\left\{1, \frac{2R\sqrt{v^2+u^2}}{Lu}\right\}. \tag{1}$$

Likewise, Wagner et al. (1999) approximate the detection probability as:

$$P_d = \begin{cases} 1 - \left(\frac{L}{R} - \sqrt{\left(\frac{v}{u}\right)^2 + 1} - 1\right)^2 \frac{R^2}{L(L-2R)} & \text{if } Rv \leq u\sqrt{L(L-2R)} \\ 1 & \text{otherwise.} \end{cases} \tag{2}$$

By calculating the area of the shaded region exactly, we calculate the detection probability without any approximations. The width w of the rectangles in Figure 4 is the vertical distance the searcher travels between turns in target-stationary geometry, or, equivalently, the distance the target travels between the searcher's turns in the original coordinate system. Hence,

$$w = u\frac{L-2R}{v} = (L-2R)\frac{u}{v}. \tag{3}$$

Depending on the width w, we may have different shapes of the areas to be calculated. Figure 6(a) shows the geometry for large w, i.e., $w > R\cos(\theta)$, where θ is the angle whose tangent is the ratio of the target's speed to the searcher's speed (see Figure 2). Figure 6(b) shows the geometry for small w, i.e., $w \leq R\cos(\theta)$. To aid our calculations in this case, we introduce angle α, where $\alpha = arcsin(w/R)$.

For large w, we can find the area of rectangle EFGH in Figure 6(a) by multiplying its width (EH) by its length (EF, which equals IK). Its width is $2R$, and its length is

$$\sqrt{w^2 + (L-2R)^2};$$

thus, its area is

$$2R\sqrt{w^2 + (L-2R)^2}.$$

The area of the two wedge-shaped regions is

$$2\left(\pi R^2 \frac{\frac{\pi}{2} - \theta}{2\pi}\right) = R^2\left(\frac{\pi}{2} - \theta\right).$$

The area of the triangular areas (e.g., triangle HIJ in Figure 6(a)) is $2(xR/2) = xR = R\cot(\theta)R = R^2\cot\theta$.

By combining these areas, we compute the probability of detection as

$$\frac{2R\sqrt{w^2 + (L-2R)^2} - R^2\cot\theta + R^2\left(\frac{\pi}{2} - \theta\right)}{wL}. \tag{4}$$

For the case when $w \leq R\cos(\theta)$, it is simplest to compute the areas ADE and BCG (which are equal by symmetry) and subtract these areas from the area of the rectangle ABCD. The area ADE can be computed by calculating the area of the trapezoid AEFD and subtracting the wedge-shaped area DEF from it.

The area of trapezoid AEFD is $(2R - R\cos\alpha)w/2$. The area of semicircle DEF is $\pi R^2(\alpha/2\pi) = R^2(\alpha/2)$. By using these, we calculate the area of region ADE as $(2R - R\cos\alpha)w/2 - R^2(\alpha/2)$.

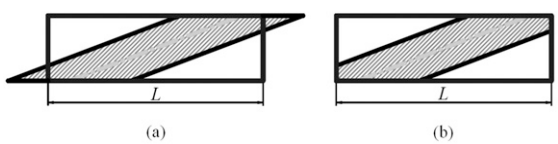

Figure 5. Approximations of the area of coverage from (a) Washburn (2002) and (b) Wagner et al. (1999).

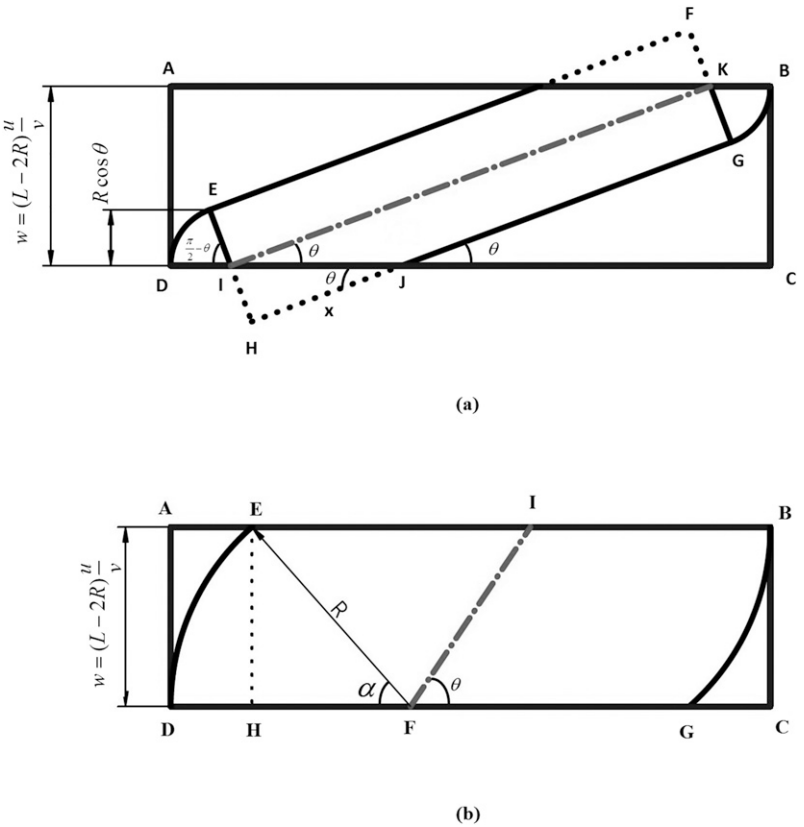

Figure 6. Qualitatively different geometries result from (a) large w and (b) small w. We handle each case separately.

Combining these areas, we compute the probability of detection as

$$\frac{wL-2\left(\frac{2R-R\cos\alpha}{2}w-R^2\frac{\alpha}{2}\right)}{wL} = 1-\frac{(2R-R\cos\alpha)w-R^2\alpha}{wL}. \quad (5)$$

Finally, in order to obtain the probability of detection for the simple border patrol problem, we combine Equations (4) and (5). Furthermore, we express each of the terms w, α, and θ as expressions of the original parameters of the problem setup: the border length L, detection radius R, target speed u, and searcher speed v. The result appears in Equation (6).

$$P_d=\begin{cases}\dfrac{2R}{L}\sqrt{\left(\dfrac{v}{u}\right)^2+1}+\dfrac{R^2v\left(\frac{\pi}{2}-\arctan\left(\frac{u}{v}\right)-\frac{v}{u}\right)}{(L-2R)uL} & \text{if}\ \dfrac{Rv^2}{(L-2R)u\sqrt{u^2+v^2}}<1\\ 1+\dfrac{R^2v\arcsin\left(\frac{(L-2R)u}{Rv}\right)}{(L-2R)uL}-\dfrac{2R}{L}+\dfrac{\sqrt{R^2v^2-(L-2R)^2u^2}}{Lv} & \text{otherwise.}\end{cases} \quad (6)$$

Figure 7 compares the detection probabilities given by Equations (1), (2), and (6) for various searcher speeds. In this figure, the border length L is 50 distance units, the detection radius R is 6 distance units, and the speed of the target u is 5 speed units (distance units/time

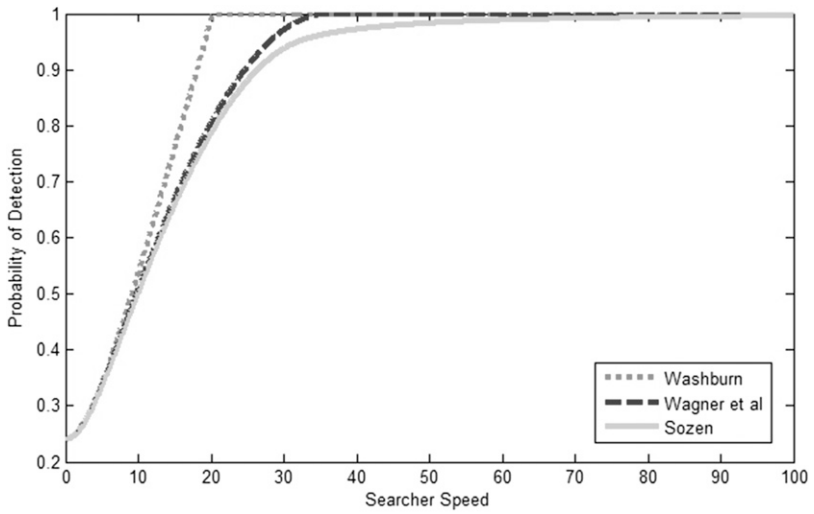

Figure 7. Comparison of detection probability formulas of Washburn, Wagner et al., and this paper.

unit). We observe that for these parameter values, the three formulas give nearly the same result for low searcher speeds. The upper bound Washburn (2002) obtained starts to differ slightly when the searcher speed is approximately twice the speed of the target. The formula of Wagner et al. (1999) starts to differ when the searcher's speed exceeds four times the target's speed. We notice from Equations (1), (2), and (6) that increasing the accuracy of the formulations increases their complexity. For simplicity, one can choose the most appropriate formula to use depending on the characteristics of a particular problem. However, it is noteworthy that both of the approximations provide optimistic estimates of the detection probability for these particular parameter values; this may be undesirable in practice.

Monte Carlo Simulation

We now examine the border patrol problem by means of a Monte Carlo simulation model. Our purpose here is twofold: first, we wish to validate our analytical formula. Second, we establish a baseline simulation model that we will augment in later sections. We use MATLAB (2012b) for all simulations. Our initial simulation setup is as follows:

1. The searcher's initial position is at a distance of R units from the left edge of the border, and its initial direction of movement is to the right.
2. We use a time-step model for our simulation. In the time-step model, we calculate the positions of the searcher and the target and make necessary computations to see if the target is detected after each time step increment. This temporal discretization introduces a small error resulting from the fact that detection may not occur at any time step, but occurs between the time steps. We choose the time step as $\Delta t = \frac{R}{25\sqrt{u^2+v^2}}$; this time step reduces the error below 6.7×10^{-3} percent. Sözen (2014) explains how the time-step is chosen and the calculation for the error. We use the same time step throughout the time-step simulations in this paper.
3. The simulation is run until the searcher makes a full cycle, i.e., comes back to its initial position and initial direction of travel. This simulation end time is referred to as $t_{\max}$.
4. Targets are generated randomly using a two-dimensional uniform distribution over a rectangle between the two barriers. Each target's initial vertical position is randomized so as to ensure that it passes through the horizontal axis of the searcher's movement before the end of the simulation. The targets' initial horizontal position is between 0 and L.
5. We simulate the movement of n targets and record the number of targets detected as k.

This approach generates the same results as generating one target and running n different simulations, however, the simulation runtime improves considerably. We then use MATLAB's ''binofit'' function to fit the Monte Carlo simulation's results to a binomial distribution, and we compute the estimated probability of detection along with its 95 percent confidence interval.

Figures 8 and 9 show the probability of detection versus the speed of the searcher when the border length L is 200 distance units, the detection radius is 6 distance units, and the speed of the target u is 5 speed units. Figure 8 shows the results of the Monte Carlo simulation with 1,000 replications, and Figure 9 shows the results of the Monte Carlo simulation with 1 million replications. In both figures, the solid line shows the probability of detection obtained from Equation (6). The dashed line shows the estimated probability of detection from the Monte Carlo simulation, and the dotted lines show the upper and lower 95 percent confidence interval of the estimated probability of detection.

From Figure 9 we can see that the estimated probability of detection obtained from the Monte Carlo matches the probability of detection obtained from Equation (6) very closely.

Recall that we assume when the searcher is R distance units away from any edge of the border, it turns in the opposite direction. Although all of the other attributes of the problem setup may be considered as fixed inputs, the turning distance is clearly within the control of the operator. Sözen (2014) studies the turning distance for 10 scenarios. In all 10 scenarios, the estimated detection probability $\widehat{P_d}$ is either insensitive to the turning distance, or it is maximized or nearly maximized at the detection radius R. Based on these results, we fix the turning distance to R for the remainder of this paper.

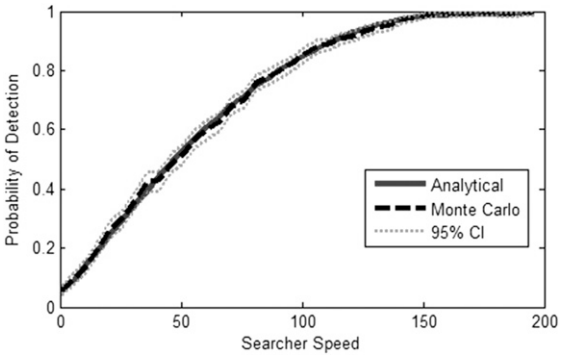

Figure 8. Comparison of the detection probability estimated from a Monte Carlo simulation with 1,000 replications and from Equation (6).

BORDER PATROL WITH MULTIPLE SEARCHERS

We now build upon the results of the previous section to study the problem of optimally employing multiple heterogeneous searchers. Our goal is to provide fundamental insights to operators of border patrol UAVs, as well as to outline a basic procedure by which an operator could perform an analysis that is suitable to his or her needs.

First, we consider the problem of optimally allocating a border among multiple searchers. If two searchers are available, the operator may either employ both searchers to patrol the entire border, or the operator may divide the border into two disjoint segments and assign each searcher to patrol one segment. We refer to the first option as the ''common path'' allocation and the second option as the ''disjoint path'' allocation.

In the following subsections we examine the probability of detection when using the disjoint and common path allocations. For simplicity, we consider only two searchers in both cases, but a similar methodology can be employed when more than two searchers are available.

Disjoint Path

Figure 10 shows the border patrol problem with two searchers and one target. The searchers allocate the border into two disjoint regions with lengths L_1 and $L_2 = L - L_1$.

Analytical Solution. The disjoint path problem in Figure 10 decomposes into two separate border patrol problems with single searchers as studied in the previous section. Based on this insight, we

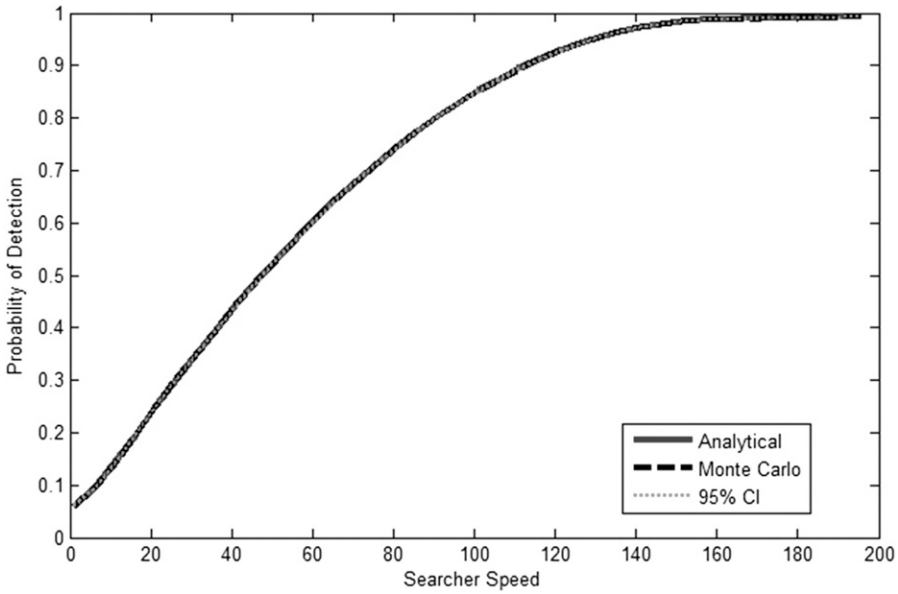

Figure 9. Comparison of the detection probability estimated from a Monte Carlo simulation with 1 million replications and from Equation (6).

compute the probability of detection using the law of total probability:

$$P_d = P_{ds1}P_{tr1} + P_{ds2}P_{tr2} \tag{7}$$

where P_{dsi} is the conditional probability that searcher i detects the target, given the target is in its region, and P_{tri} is the probability that the target is in the region of searcher i.

We can compute P_{dsi} by substituting the appropriate values for searcher i into Equation (6):

$$P_{dsi} = P_d(L_i, R_i, u, v_i). \tag{8}$$

Since we assume that the horizontal position of the target is uniformly distributed along the border, we have $P_{tri} = L_i/L$. Thus, we have

$$\begin{aligned} P_d &= P_{ds1}\frac{L_1}{L} + P_{ds2}\frac{L_2}{L} \\ &= P_d(L_1, R_1, u, v_1)\frac{L_1}{L} + P_d(L_2, R_2, u, v_2)\frac{L_2}{L}. \end{aligned} \tag{9}$$

In general, with n searchers and one target, we have

$$P_d = \sum_{i=1}^{n} P_{dsi}\frac{L_i}{L} = \frac{1}{L}\sum_{i=1}^{n} P_d(L_i, R_i, u, v_i)L_i. \tag{10}$$

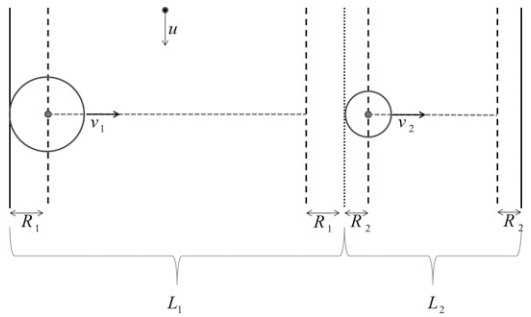

Figure 10. Problem setup for the disjoint path allocation.

Monte Carlo Simulation. We also evaluate the disjoint path problem by means of a Monte Carlo simulation. The following setup applies to our simulation:

1. The searchers' initial positions depend on their detection radii and their allocated regions. The initial position of the ith searcher is distance R_i away from the edge of its allocated region. Its direction of movement is toward the opposite edge, and its turning distance is R_i distance units from the end of its allocated region. If $R_i \geq L_i/2$ for any searcher, the searcher remains stationary at

the midpoint of its allocated region. (In practice, a fixed-wing UAV could not remain truly stationary and would need to execute a loiter pattern. It may be possible for a rotary-wing aircraft or lighter-than-air UAV to remain stationary.)

2. Recall that in the single searcher case, we run our simulation until the searcher arrives at its initial starting position. Depending on the allocated regions and characteristics of the searchers, such a policy may result in a very long runtime in the disjoint path case. Thus, we limit our simulation end time to 25 times the maximum time required for any searcher to make a full cycle in its allocated region. Sözen (2014) explains the rationale for this choice of multiplier.
3. We generate targets and calculate detection probabilities as in the previous section.

Figure 11 shows the probability of detection P_d as calculated analytically using Equation (9), as well as the estimated value $\widehat{P_d}$ as determined via Monte Carlo simulation with one million replications. Detection probability is expressed as a function of the ratio of the border length allocated to the first searcher, L_1, to the total border length L. This ratio is varied from 0 to 1 with 0.01 increments. In this specific case L is 200 distance units, detection radii R_1 and R_2 are 12 and 6 distance units, respectively; the target speed u is 5 speed units, and the speeds of the searchers, v_1 and v_2, are each 20 speed units.

Comparing the analytical solution to the Monte Carlo simulation, we see a discrepancy at very high or low values of L_1/L. When L_1/L is very large or very small, this means that the region allocated to one of the searchers is very small. Figure 12 shows the case when the region allocated to the first searcher is very small. In this case we have $R_1 > L_1/2$, so the first searcher remains in the middle of its allocated region and covers some portion of the area allocated to the second searcher. This extra region is shaded with horizontal stripes in Figure 12 and is not accounted for in the analytical solution. Because of this extra region, the Monte Carlo simulation produces a higher detection probability value than the analytical solution when the allocation to any searcher is less than two times the detection radius of that searcher.

Common Path

Figure 13 shows the border patrol problem with two searchers sharing the same path and attempting to detect a single target. Although

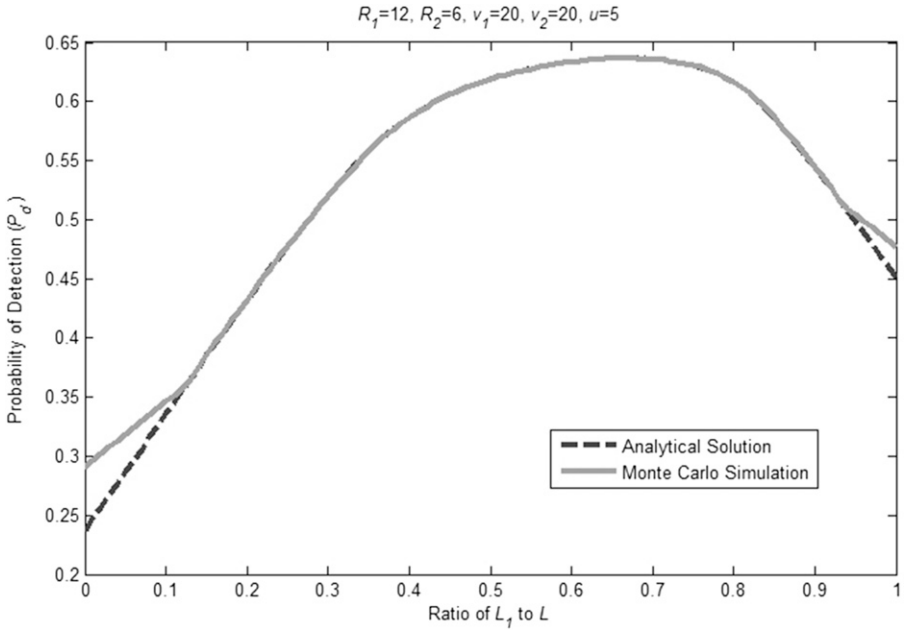

Figure 11. Detection probability utilizing a disjoint path allocation.

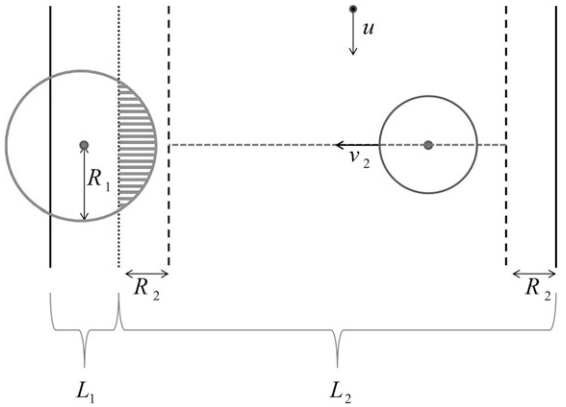

Figure 12. Disjoint path extreme case.

the searchers share the same path, their turning points may differ due to their differing detection radii. For clarity, we introduced a slight vertical displacement in the paths that the searchers follow, although in reality we assume that there is no vertical displacement.

The common path allocation is difficult to evaluate analytically; thus, we utilize Monte Carlo simulation to analyze it. Our simulation in this section is based on the Monte Carlo simulation for the disjoint path case, with modifications to the searchers' initial positions and their turning points.

The initial starting point of the searchers could be chosen to be the same point, i.e., they could initially start their movement from exactly the same location. However, if their detection radii and speeds were identical, then they would move together and would perform no better than a single searcher. For this reason, we choose to initialize searcher i's location as $L(i-1)/n + R_i$, where n is the number of searchers. The searchers' initial direction of movement is toward the right. As before, each searcher's turning distance is simply its detection radius. Figure 14 shows our initial setup for the common path simulations; dashed lines show the turning points of the searchers.

The simulation is run until all searchers come back to their initial starting point. In order to reduce the runtime, the simulation end time is limited to 100 times the maximum time it takes for any searcher to make a full cycle.

We perform one million Monte Carlo simulations for the common path case with the same searcher and target variable settings we considered in the disjoint path problem (Figure 11). We obtain an estimate and 95 percent confidence interval for the probability of detection. This estimate is shown in Figure 15, along with the results previously obtained for the disjoint path case. (Due to the large number of replications, the confidence interval is difficult to detect in the figure.)

Since there is no allocation of borders in the common path problem, the estimated probability of detection is constant. It is plotted over the results from Figure 11 in order to provide a comparison between the disjoint and common path allocations.

Figure 15 shows that the common path detection probability is higher than the disjoint path probability for nearly half of the L_1/L values. This means that if we do not allocate the border to the two searchers properly for the disjoint path case, we may end up with

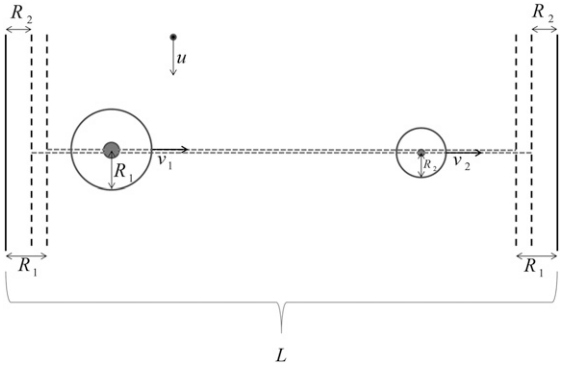

Figure 13. Problem setup for the common path allocation.

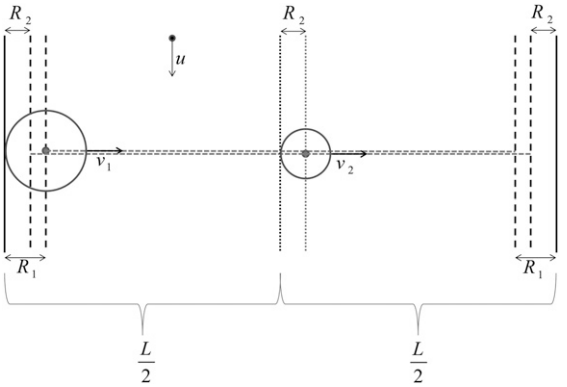

Figure 14. Searchers' initial positions and movement vectors in the common path simulations.

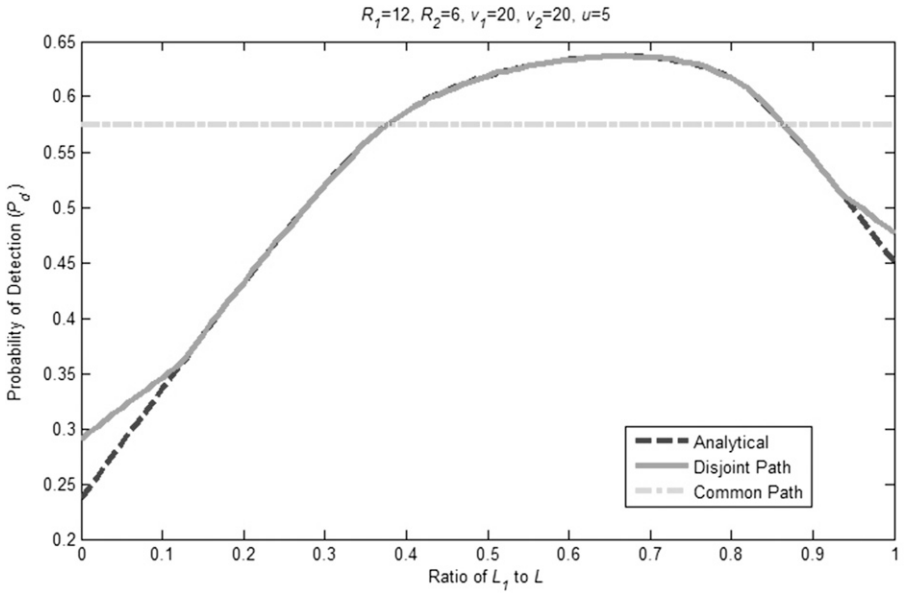

Figure 15. Common path Monte Carlo simulation results.

a worse probability of detection than we would obtain without allocating the region at all. However, by intelligently allocating the border, we are able to obtain a higher detection probability than is possible with the common path allocation. We now consider the problem of optimally allocating the border so as to maximize detection probability.

OPTIMAL ALLOCATION OF REGIONS

In this section we wish to determine an optimal allocation of a border between two searchers. Although we consider only two searchers, our general approach can be extended to accommodate $n > 2$ searchers.

In the optimal allocation problem, our goal is to determine L_1 and L_2 such that the overall probability of detection is maximized. That is, given values for L, R_1, R_2, u, v_1, and v_2, we wish to determine L_1 and L_2 such that $L_2 = L - L_1$ and the probability of detection is maximized:

$$\max_{L_1} \quad P_d(L_1, R_1, u, v_1)\frac{L_1}{L} + P_d(L - L_1, R_2, u, v_2)\frac{L - L_1}{L} \quad st\ 0 \le L_1 \le L \tag{11}$$

This is a constrained optimization problem with one decision variable and a convex feasible region. The concavity of the objective function, given by Equation (9), is difficult to evaluate analytically. Sözen (2014) performed an extensive computational evaluation and was unable to find a counterexample showing that the objective function is nonconcave, thus raising the possibility of finding a globally optimal solution by locating a stationary point of the objective function. However, other good methods for solving the above optimization problem include conducting a line search on L_1 and evaluating potential allocations by means of a simulation model.

Monte Carlo Simulation

We now perform a Monte Carlo simulation study to compare various border allocations to a common path approach for a variety of scenarios. Specifically, we vary the detection radii and speeds of the searchers while fixing the length of the border to 200 distance units and the speed of the target to 5 speed units. In each scenario, we vary the allocation of border to the first searcher in 1 percent increments, each with one million replications, in order to observe the change in the probability of detection. We then compare this detection probability to the detection probability obtained by a common path solution.

Figure 16 illustrates the outcome of six representative setups. Each subfigure in Figure 16 is generated with the same logic as Figure 15,

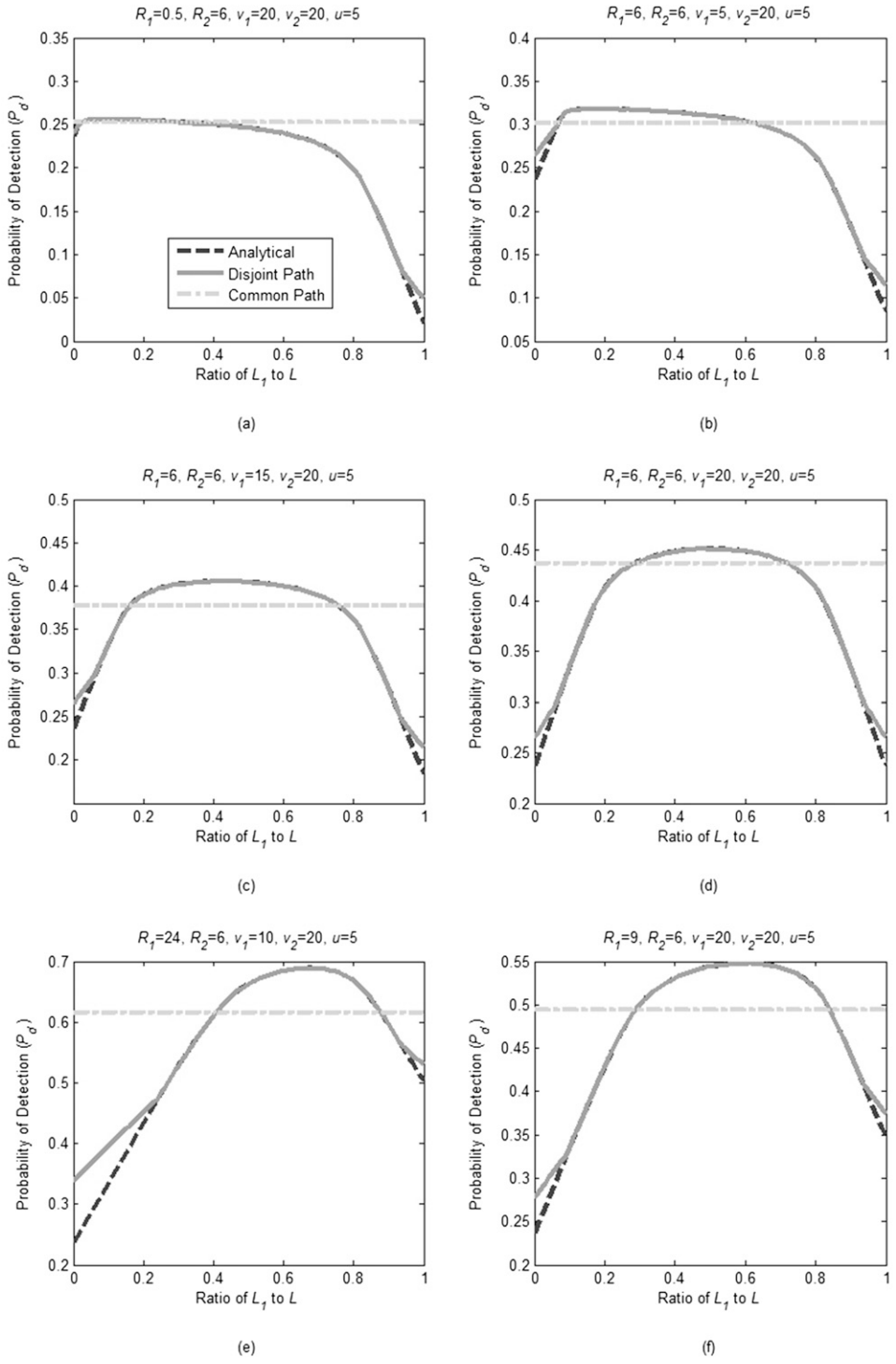

Figure 16. Monte Carlo simulation results for various searcher characteristics.

where the subfigures show the probability of detection versus the fraction of the border allocation to the first searcher. The dashed line shows the analytical disjoint path detection probability (Equation (9)), the solid line shows the estimated probability of detection for the disjoint path case obtained from the Monte Carlo simulation, and the dashed-dotted line shows the estimated probability of detection for the common path case obtained from the Monte Carlo simulation. We also plotted 95 percent confidence intervals for the estimated probabilities of the common path and disjoint path cases, but due to the large number of replications, they are difficult to detect in the figures.

In Figure 16(a) we see that the optimal allocation to the first searcher is very low since its detection radius is inferior to that of the second searcher, while their speeds are equal to each other. It is also interesting to note that the optimal detection probability is very close to the common path probability of detection. This occurs because the optimal allocation to the second searcher is nearly the entire border.

In Figure 16(b), the first searcher's capabilities are still inferior to those of the second searcher, but not as much as in Figure 16(a). Thus, more of the border is allocated to the first searcher. The difference between the common path probability and optimal allocation probability has also increased. Further increasing the speed of the first searcher (Figure 16(c)), results in a further increase in its allocation, and the gap between the common path and optimal allocation probability widens.

When we increase the speed of the first searcher such that the properties of both searchers are equal, we expect to have the same border allocation to both searchers. We might also expect to see a larger gap between the common path and optimal allocation probabilities compared to the previous cases. As Figure 16(d) indicates, our first expectation is correct, but our second is not. This occurs mainly because of improved performance in the common path case. In particular, when the two searchers have the same characteristics, they can operate in a cyclical fashion. Specifically, the two searchers cross each other at the same place every time they transit the border. These crossings occur when they are moving in opposite directions, causing them to have relatively brief overlap periods. Shorter crossing times means less coincident area covered by the searchers, resulting in a smaller gap between the common path and optimal allocation probabilities.

In Figure 16(e) and Figure 16(f) one searcher is inferior, but by a smaller margin than in Figure 16(a) though Figure 16(c). The differences between the common path and optimal allocation probabilities are larger here than the other four scenarios.

In general, we observe that if one of the searchers is superior to the other, the allocation of the border to the inferior searcher is low, and the difference between the common path and optimal allocation probabilities is lower than one might expect. Decreasing the difference in the capabilities of the searchers results in a higher allocation to the inferior searcher and can widen the gap between the common path and optimal allocation probabilities. However, due to the perfect coordination between the searchers when the searchers have the same characteristics, the gap between the common path and optimal allocation probabilities can be low in some cases.

Based on our results, we conclude that the best possible detection probability is obtained by an optimal implementation of the disjoint path approach. However, if a user cannot determine the optimal allocation, or if the characteristics of the searchers are unknown or subject to change, the user may choose the common path approach in order to avoid the risk of choosing a poor allocation. If the common path is utilized, the UAVs should be employed in such a way as to reduce the time when they pass or cross each other to further increase the detection probability.

Varying Detection Radius as a Function of Speed

In practice, it is likely that the detection capability of a searcher depends on its speed. For example, with a vision-based sensor, the quality of the video would be reduced if the UAV were to travel at a very fast speed. In this subsection, we model this degradation in sensor quality as a reduction in detection radius. We now consider the problem of selecting optimal speeds and allocations of our searchers when

their detection radii vary as a function of speed.

Single Searcher. As before, we first consider a single searcher. In order to make a comparison with the constant detection radius case (Figure 9), we utilize the same parameters as before, with the exception of the detection radius. We model the detection radius as a monotonically decreasing function of the searcher speed; in particular, we choose $R = 6e^{-v/60}$. The same approach could be employed for a different sensor model.

Figure 17 shows the detection radius as a function of speed (left) and the corresponding probability of detection (right). As the figure indicates, the probability of detection first increases with increasing speed; then it starts to decrease after reaching a maximum.

In general, the probability of detection increases with both increasing speed and increasing detection radius. However, when detection radius decreases with increasing speed, the performance benefit obtained from a higher speed must be weighed against the impairment caused by a smaller detection radius. For the particular example in Figure 17, at lower speeds, the probability of detection increases with increasing searcher speed. After the maximum probability of detection point, effect of decreasing detection radius dominates the effect of increasing speed.

Multiple Searchers. We now consider joint selection of speed and border allocation in the two-searcher problem. For our computational experiments we consider the same border length and target speed as in the previous case; in particular, we have $L = 200$ and $u = 5$ units. For simplicity, we hold one searcher's detection radius constant at 6 units while allowing the other searcher's detection radius to vary as a function of its speed. In particular, we let $R_1 = 6e^{-v_1/60}$ and set the speed of the second searcher to 100 speed units. Then, we vary the speed of the first searcher and observe the optimal allocation and the probability of detection at the optimal allocation.

We can see in Figure 18(a) that the allocation to the first searcher starts with 0.06 when its speed is 0; in other words, when it is stationary. An allocation of 0.06 means that $0.06 \times 200 = 12$ units are allocated to the first searcher, which is double its detection radius when it is stationary. In this case, the probability of detection of the first searcher in its region is 1.

Although increasing v_1 decreases R_1, the optimal allocation to the first searcher nevertheless increases as v_1 increases from zero. After some point ($v_1 = 57.2$ in Figure 18(a)) the optimal allocation to the first searcher starts to decrease.

We have a similar relationship for the probability of detection as a function of the speed of the first searcher. When we start with the first searcher being stationary and increase

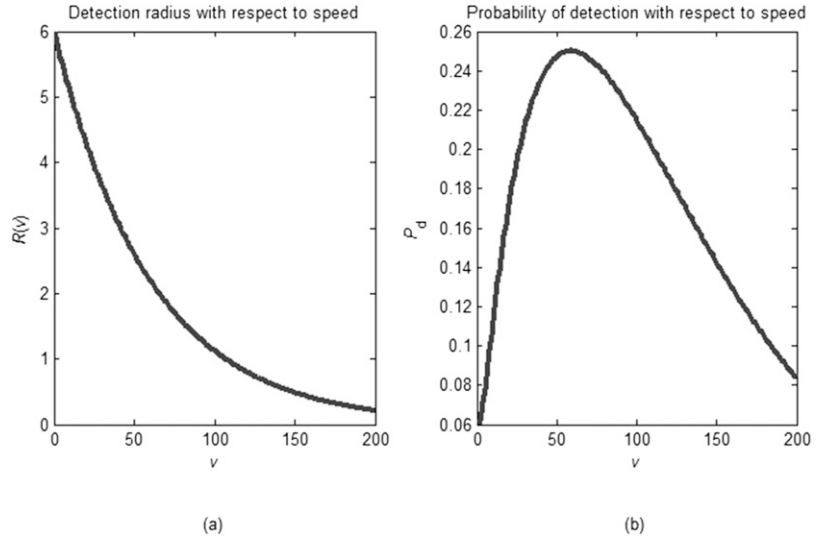

Figure 17. Impact of varying detection radius as a function of speed.

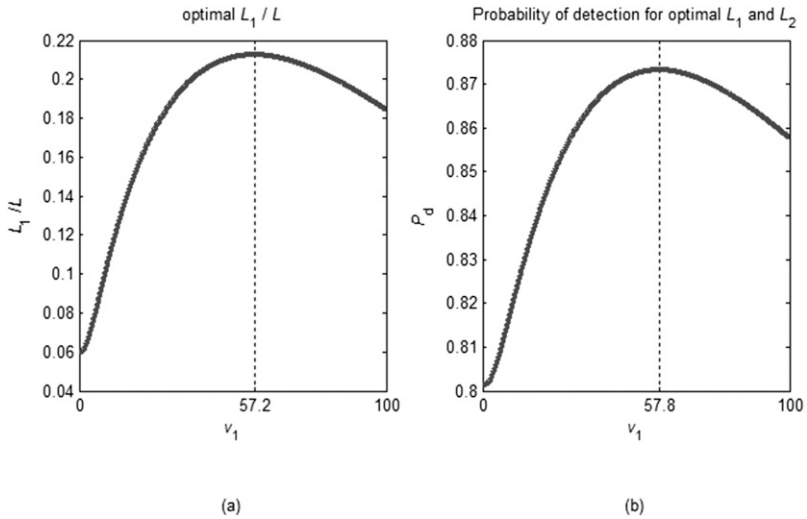

Figure 18. Optimal border allocation and detection problem when the first searcher's detection radius varies as a function of speed.

v_1 infinitesimally, we notice a reduction in the probability of detection. Further increasing v_1 results in an increase. This behavior shows that the probability of detection for this problem is non-concave. Further increasing v_1 causes a reduction in probability of detection after $v_1 = 57.8$. Interestingly, the peaks of two curves in Figure 18(a) and Figure 18(b) do not occur at the same v_1. That is, the speed that results in the largest allocation to the first searcher is not the speed that results in the highest aggregate detection probability. This phenomenon persists across varying problem parameters.

Multiple Searchers with Varying Detection Radii Depending on Speed. We now consider the case in which the detection radii of both searchers are functions of their corresponding speeds. We use the same function for the detection radius of the first searcher that we used previously, $R_1 = 6e^{-v_1/60}$, and we use a slightly different function for the second searcher in order to observe the difference in the results. Specifically, we use $R_2 = 6e^{-v_2/90}$. These functions appear in Figure 19.

Figure 20(a) shows the optimal allocation to the first searcher with searcher speeds varying from 0 to 100 speed units in increments of 0.1 units. For each searcher speed setting, the detection probability resulting from an optimal allocation appears in Figure 20(b).

As Figure 17 indicates, when one searcher is stationary its allocation is equal to twice its detection radius. In the region where both searchers have moderate speeds, increasing v_1 up to around 60 speed units while keeping v_2 constant results in an increase in the optimal allocation to the first searcher and in the probability of detection. After that value, both the allocation to the first searcher and the detection probability start to decrease. This is not the case for v_2. When v_1 is kept constant and v_2 is increased up to around 70 speed units, the allocation to the first searcher decreases, which means that the allocation to the second searcher increases. After that value, the

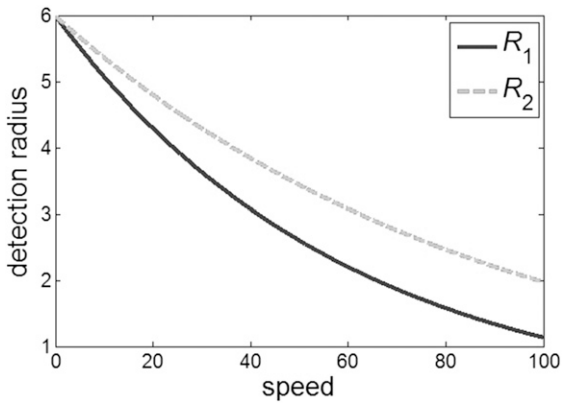

Figure 19. Detection radii of the two searchers.

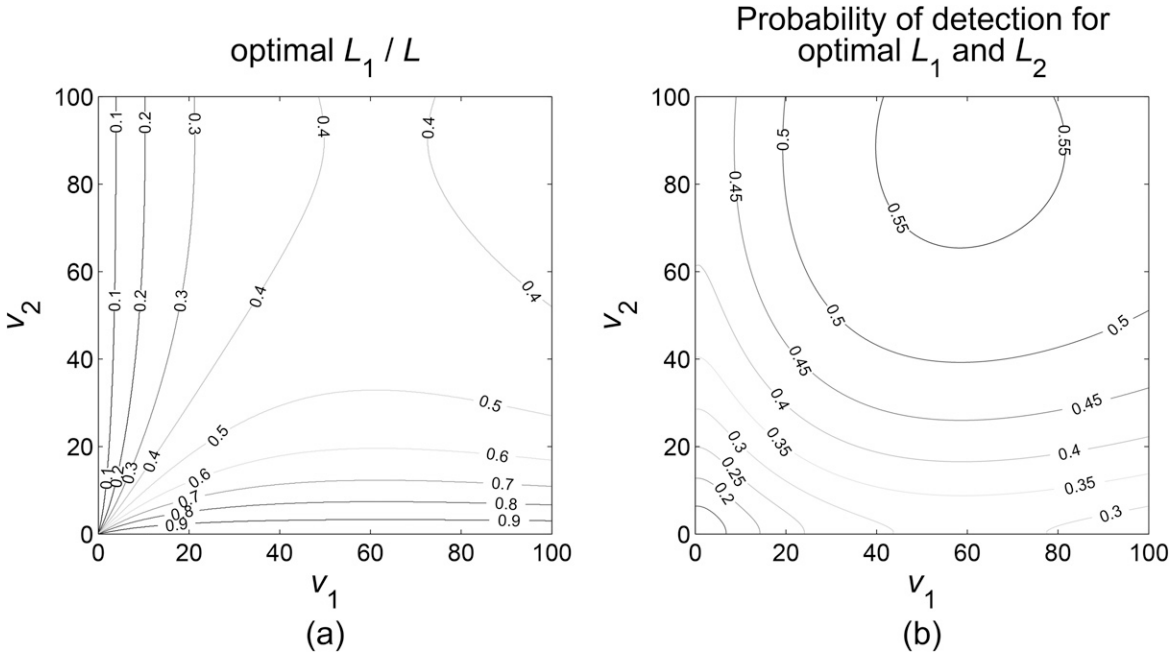

Figure 20. Impact of varying both searchers' detection radii.

allocation stays nearly constant. However, the detection probability continues to increase. This can be understood by noting that the detection radius of the second searcher does not decrease as much as that of the first searcher. The positive effect of increasing the second searcher's speed tends to dominate the negative effect of the reduction in the detection radius for speeds up to 100 speed units for the second searcher. For this particular case, the maximum probability of detection is 56 percent which is achieved when $v_1 = 58.3$ and $v_2 = 88.4$ speed units. At these speed values, the optimal allocation to the first searcher is about 40 percent of the border length.

SUMMARY

This paper develops both analytical and Monte Carlo simulation models for the simple border patrol problem in which a single searcher equipped with a cookie cutter sensor patrols a straight border to detect intruders. Our analytical formula improves the detection probabilities computed in the literature by using highly accurate geometrically-based calculations.

After computationally verifying our models for the simple border patrol problem, we add complexity to the problem by introducing another searcher. We propose two different strategies for the multiple-searcher problem: the disjoint path and the common path allocation. We develop both analytical and Monte Carlo simulation models for the disjoint path problem by building upon the single searcher case. We also develop a Monte Carlo simulation model for the common path problem.

When we compare the results of the two multiple-searcher cases, we see the importance of optimally allocating the border to the two searchers. Although the disjoint path deployment can provide a better detection probability than the common path, it is important to allocate the border intelligently between the two searchers. Otherwise, the detection probability may be worse than that resulting from a common path deployment.

We also analyze the effect of degrading detection performance with increasing searcher speed. We perform an analysis for a single

searcher, then extend this analysis to multiple-searcher problems. Besides analyzing the speeds that result in maximum detection probability, we determine the optimal allocation to maximize the detection probability.

REFERENCES

Eagle, J. 2013. Search and Detection Theory. Lecture notes, course OA3602, Naval Postgraduate School, Monterey, CA (September 27).

Girard, A. R., Howell, A. S., and Hedrick, J. K. 2004. Border Patrol and Surveillance Missions Using Multiple Unmanned Air Vehicles, *Proceedings 43rd IEEE Conference on Decision and Control*, Atlantis, Paradise Island, Bahamas.

Haddah, C. C., and Gertler, J. 2010. *Homeland Security: Unmanned Aerial Vehicles and Border Surveillance.* CRS Report No. RS21698, Congressional Research Service; http://www.fas.org/sgp/crs/homesec/RS21698.pdf (accessed August 20, 2016).

Matveev, A. S., Teimoorib, H., and Savkinb, A. V. 2011. A Method for Guidance and Control of an Autonomous Vehicle in Problems of Border Patrolling and Obstacle Avoidance, *Automatica*, Vol 47, No 3, 515–524.

Ozcan, B. Y. 2013. *Effectiveness of Unmanned Aerial Vehicles in Helping Secure a Border Characterized by Rough Terrain and Active Terrorists.* Master's thesis, Naval Postgraduate School, Monterey, CA.

Preston, J. 2014. Border Patrol Seeks to Add Digital Eyes to Its Ranks, *New York Times* (March 21); http://www.nytimes.com/2014/03/22/us/border-securitys-turn-toward-the-high-tech.html.

Soza & Company. 1996. *The Theory of Search: A Simplified Explanation.* Report, US Coast Guard Office of Search and Rescue; http://www.navcen.uscg.gov/pdf/theory_of_search.pdf (accessed August 20, 2016).

Sözen, V. 2014. Optimal Deployment of Unmanned Aerial Vehicles for Border Surveillance. Master's thesis, Naval Postgraduate School, Monterey, CA.

Szechtman, R., Kress, M., Lin, K., and Cfir, D. 2007. Models of Sensor Operations for Border Surveillance, *Naval Research Logistics*, Vol 55, No 1, 27–41.

Wagner, D. H., Mylander, W. C., and Sanders, T. J., eds. 1999. *Naval Operations Analysis.* Naval Institute Press.

Washburn, A. R. 2002. *Search and detection.* INFORMS.